Predicting object slippage in robotic grippers using human-inspired tactile processing

Giuseppe Vitrani[1] and Michaël Wiertlewski[1]

***Abstract*— Humans can continuously perceive and react to an object slipping from grasp using touch. The detection of slippage is independent of the object properties and occurs in hundreds of milliseconds. To achieve this performance it has been postulated that the nervous system seeks stereotypical patterns of deformation to rapidly detect object slippage regardless of the friction coefficient. In comparison, robotic tactile sensors currently offer limited capability in estimating slip sensation, as they are often unable to detect slip precursors and only respond once a full slip occurs. Here, we show a method to estimate how far away from full slip the contact is by projecting tactile data on a low-dimensional space. This space is built by extracting the principal components of the pressure distributions found using the Cattaneo-Mindlin model. This approach, inspired by human behavior, can quickly and robustly estimate the degree of slip of an object grabbed by a robotic gripper.**

I. INTRODUCTION

The gradual slippage of an object, also called as *incipient slip* is a central information provided by the sense of touch to enable safe and delicate grasping. By detecting incipient slip, controllers can prevent sudden object fall while minimizing the grasping force, which is crucial to handle fragile objects [1], [2].

Remarkably, humans can detect slip from the deformation of the skin detected from the thousands of mechanoreceptors regardless of the specific properties of the object in hand. It is unclear however, how humans can process such a vast amount of sensory afferent so rapidly. A possible explanation lies in the *Efficient Coding Hypothesis*, presented for the first time by Horace Barlow in [3]. According to this hypothesis, the transmission of sensations from sensory organs (e.g. fingertip) to the nervous system uses a compact representation of stimuli to compress the information and reduce redundancy. In the specific case of human touch, Willemet et al. suggested that only six fingertip strain patterns were enough to perceive incipient slip independently of the frictional conditions [4].

In comparison, the tactile slip perception implemented in robotic grasping is by far more limited [5]. In many cases, the gradual nature of the phenomenon is ignored and only gross slip is detected [6], [7], [8]. Even when a degree of slip is estimated, it depends on the specific material or object properties, without a clear method to generalize [9], [10]. The limits of these methods apply even for high-resolution tactile sensors, which suggests that a proper processing of tactile data is as important as hardware advancements when it comes to interpreting physical phenomena such as the incipient slip.

[1]Delft University of Technology, Cognitive Robotics Department, 2628 CD, Delft, The Netherlands `g.vitrani@tudelft.nl`

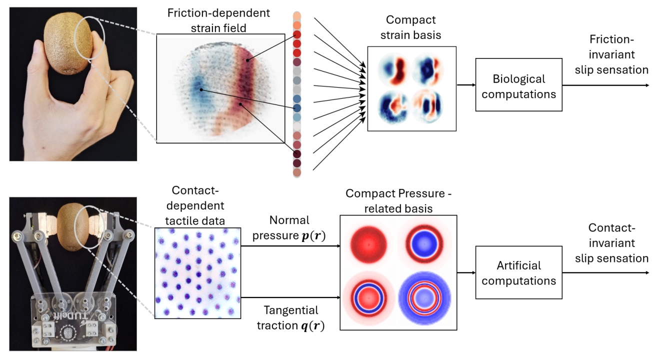

Fig. 1. Bioinspired slip processing schematic. Partially adapted from [4].

In this work, we discuss a processing framework based on contact mechanics to extract the degree of object slippage from tactile data (Fig. 1). The dimensionality of the distribution of normal pressure $p(r)$ and tangential traction $q(r)$ can be reduced to few main components that highly correlate with the evolution of slip. By assessing the activation of these components, an off-the-shelf classifier can robustly estimate the degree of slippage under variable contact conditions.

II. METHODOLOGY

A. Analytical contact model

We developed an analytical model of sliding contact based on Hertz and Cattaneo-Mindlin theories [11] to simulate the tactile interaction between an hemispheric soft sensor (with radius R_1 = 10mm, Young and Poisson ratio being $E_1 = 0.5$ MPa and ν_1 =0.45 respectively) pressed on a flat or curved surface (i.e. sphere vs sphere). We were interested in the distribution of normal pressure p and tangential traction q on the contact area a. In the simulated cases, a was always circular while $p(r)$ and $q(r)$ are axisymmetric. We defined $\alpha(r) = \arctan \frac{q(r)}{p(r)}$ as the angle formed between the localized normal and tangential forces, implying that in the sliding portion of the contact area μ is equal to $\tan(\alpha(r))$.

As a measure of the degree of incipient slip, we use the *Safety Margin* (Γ), defined as $\Gamma = \frac{Q^* - Q}{Q^*}$, where Q^* is the critical tangential force when slippage occurs and Q is the current one. Γ ranges from 0 (gross slippage reached) to 1 (no tangential forces are applied).

B. Data generation

Dataset consisting of about 16000 samples from variable contact conditions were generated for $p(r)$, $q(r)$ and $\alpha(r)$.

Combinations of object stiffness (i.e. E_2,ν_2), curvature R_2, friction coefficient μ, and normal force P were extracted randomly from predefined intervals defined as follows:

- P ranging from 1 to 5 N. Forces above 5 N were avoided to prevent the contact area from being too big.
- μ ranging from 0.1 to 0.9.
- R_2 ranging from 10 to 50 mm or flat.
- E_2,ν_2 defined the material stiffness. Half of the simulations were performed considering stiff surfaces, with E_2 and ν_2 ranging from 100 to 300 GPa and 0.2 to 0.3 respectively. The other half of the simulations featured softer materials similar to the one assumed for the sensor, with E_2 and ν_2 ranging from 0.1 to 10 MPa and 0.35 to 0.45 respectively.

The tangential force Q was increased until full slippage was reached, resulting in Γ ranging from 1 to 0 for each different combination of parameters. The acquired data were organized in matrix form, resulting in X_p,X_q and X_α, consisting of n =10000 rows (i.e. flattened 100x100 2D contact data grid) and m =16000 columns (i.e. number of samples). Noise drawn from a uniform distribution within the range $\pm maxvalue$ of each contact data distribution was added. From now, we will consider only X_α, as the results and considerations for X_q are totally similar.

C. Data analysis

We found a low-dimensional structure of Γ using the Singular Value Decomposition (SVD) on X_α. A schematic representation of the process can be seen in Fig.2.

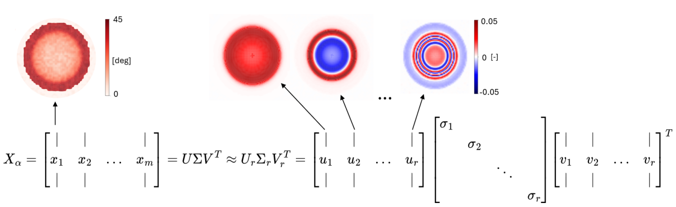

Fig. 2. Schematic representation of the SVD applied to X_α.

By keeping only a limited amount of r columns of U, Σ and V^T, we can achieve a rank-r approximation of X_α. We are interested in the columns of U_r, containing the dominant X_α singular values u_k, hierarchically arranged.

III. RESULTS AND DISCUSSION

A. Low-Dimensional structure of slip

Despite the contact variability injected in X_α, just 8 singular values (i.e. r=8) are sufficient to explain more than 95% of the variance in the data. Particularly, the first three bases u_1, u_2, and u_3 explain 72%, 11%, and 5% of the variance respectively, and together they explain approximately 88% of the variance of X_α.

To evaluate if these 8 singular values provide a compact representation of Γ, every simulation of X_α was projected on these eight principal values, to compute the activation of these main bases. We visualize the dataset by showing the projections of all the columns in X_α on the first three principal components, resulting in the scatter plot shown in Fig.3. The safety margin Γ is encoded in the color.

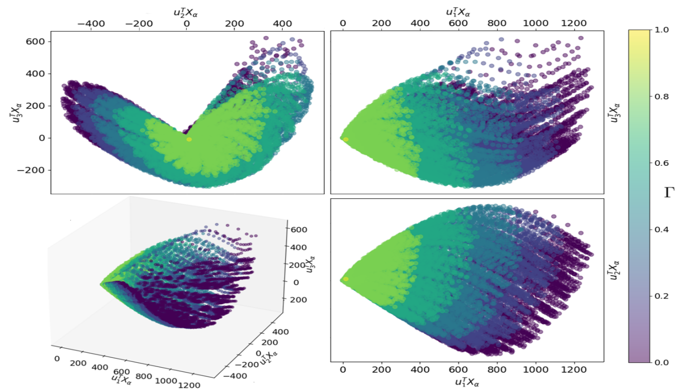

Fig. 3. Projection of X_α columns on u_1, u_2 and u_3 (i.e. $u_1^T X_\alpha$, $u_2^T X_\alpha$ and $u_3^T X_\alpha$, respectively) . The slip degree Γ clusters regularly on this low-dimensional space.

The distribution of Γ for all contact conditions clusters regularly in this low-dimensional 3D space, with the projections gradually approaching the axis origin as $\Gamma \rightarrow 1$.

B. Slip degree classification

To evaluate the advantages of a low-dimensional representation of the Γ, we used a simple k-nearest neighbors (KNN) classifier with $k = 5$. X_α was split considering 70% of the data for training, while the remaining 30% was used for testing. We wanted to predict five classes of Γ, ranging from 1-0.8, 0.8-0.6, 0.6-0.4, 0.4-0.2, 0.2-0. We compared on one side the effect of taking the whole dataset columns as a classifier input or on the other side, only considering the projection of such columns on an increasing number of bases. Specifically, we trained a KNN considering the full columns of X_α (i.e. 10000 input size, from the 100x100 original grid) and we consider the projections of each X_α column on an increasing number of u_k, up to 100. In Fig.4 are shown the test accuracy results for these two cases in red and blue respectively, with emphasis on the first 8 u_k.

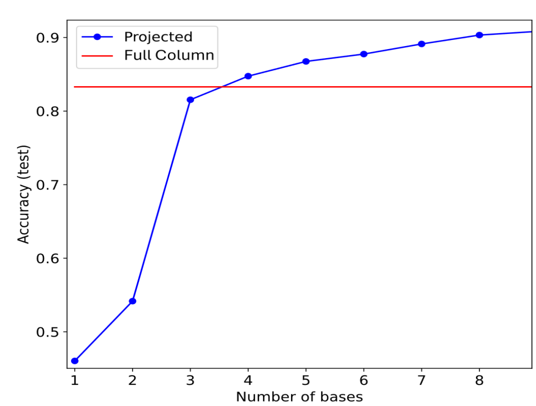

Fig. 4. KNN test accuracy: entire X_α columns (red) vs projection of X_α columns on an increasing number of bases (blue).

These results show that the first three singular values are sufficient to achieve an overall accuracy of 81%, which is close to the one using the full X_α columns, i.e. 83%. Instead, the accuracy obtained by recruiting eight singular values reaches around 91%. From the 9th base on, the increase in accuracy is negligible.

IV. CONCLUSIONS AND FURTHER WORK

These results suggest that a compact and physics-based representation of Γ can be achieved, hence creating a more robust estimation of slip for objects with unknown properties or in presence of measurement noise, while promoting computational efficiency. This approach takes inspiration from the human-like processing of slip, where the assessment of the degree of slip is likely based on the recognition of few deformation patterns. Indeed, these preliminary results are well aligned with the efficient coding hypothesis and the results presented by Willemet et al. [4] in the human case. Future work will cover the experimental validation of the approach. These results have repercussions for reactive grippers that can modulate their grip force in response to frictional conditions.

REFERENCES

[1] R. S. Johansson and G. Westling, "Signals in tactile afferents from the fingers eliciting adaptive motor responses during precision grip," *Experimental brain research*, vol. 66, pp. 141–154, 1987.

[2] A.-S. Augurelle, A. M. Smith, T. Lejeune, and J.-L. Thonnard, "Importance of cutaneous feedback in maintaining a secure grip during manipulation of hand-held objects," *Journal of neurophysiology*, vol. 89, no. 2, pp. 665–671, 2003.

[3] H. B. Barlow *et al.*, "Possible principles underlying the transformation of sensory messages," *Sensory communication*, vol. 1, no. 01, pp. 217–233, 1961.

[4] L. Willemet, N. Huloux, and M. Wiertlewski, "Efficient tactile encoding of object slippage," *Scientific Reports*, vol. 12, no. 1, p. 13192, 2022.

[5] W. Chen, H. Khamis, I. Birznieks, N. F. Lepora, and S. J. Redmond, "Tactile sensors for friction estimation and incipient slip detection—toward dexterous robotic manipulation: A review," *IEEE Sensors Journal*, vol. 18, no. 22, pp. 9049–9064, 2018.

[6] S. Dong, W. Yuan, and E. H. Adelson, "Improved gelsight tactile sensor for measuring geometry and slip," in *2017 IEEE/RSJ International Conference on Intelligent Robots and Systems (IROS)*. IEEE, 2017, pp. 137–144.

[7] S. Dong, D. Ma, E. Donlon, and A. Rodriguez, "Maintaining grasps within slipping bounds by monitoring incipient slip," in *2019 International Conference on Robotics and Automation (ICRA)*. IEEE, 2019, pp. 3818–3824.

[8] P. M. Ulloa, D. C. Bulens, and S. J. Redmond, "Incipient slip detection for rectilinear movements using the papillarray tactile sensor," in *2022 IEEE Sensors*. IEEE, 2022, pp. 1–4.

[9] W. Yuan, R. Li, M. A. Srinivasan, and E. H. Adelson, "Measurement of shear and slip with a gelsight tactile sensor," in *2015 IEEE International Conference on Robotics and Automation (ICRA)*. IEEE, 2015, pp. 304–311.

[10] R. Sui, L. Zhang, T. Li, and Y. Jiang, "Incipient slip detection method with vision-based tactile sensor based on distribution force and deformation," *IEEE Sensors Journal*, vol. 21, no. 22, pp. 25 973–25 985, 2021.

[11] K. L. Johnson and K. L. Johnson, *Contact mechanics*. Cambridge university press, 1987.